Thermodynamic Properties of Layered Tetradymite-like Compounds of the Ag–Ge–Sb–Te System

Moroz, M.; Tesfaye, Fiseha; Demchenko, P.; Prokhorenko, M.; Lindberg, D.; Reshetnyak, O.; Hupa, Leena

[Link to publication](#)

Please cite the original version:
Moroz, M., Tesfaye, F., Demchenko, P., Prokhorenko, M., Lindberg, D., Reshetnyak, O., & Hupa, L. (2020). Thermodynamic Properties of Layered Tetradymite-like Compounds of the Ag–Ge–Sb–Te System. In J. Lee, S. R. Wagstaff, G. Lambotte, A. Allanore, & F. Tesfaye (Eds.), *Materials Processing Fundamentals 2020* (pp. 275–287). (Minerals, Metals and Materials Series). Springer. https://doi.org/10.1007/978-3-030-36556-1_23

Thermodynamic Properties of Layered Tetradymite-like Compounds of the Ag–Ge–Sb–Te System

Mykola Moroz,[✉] Fiseha Tesfaye, Pavlo Demchenko, Myroslava Prokhorenko, Daniel Lindberg, Oleksandr Reshetnyak, Leena Hupa

Abstract

The phase equilibria of the Ag–Ge–Sb–Te system in the part Ag_8GeTe_6–Ge–GeTe–Sb_2Te_3 were investigated by the electromotive force (EMF) method. The determined phase relations were used to express the chemical reactions. The potential-forming reactions were performed by applying electrochemical cells (–) C | Ag | Ag_2GeS_3-glass | D | C (+), where C is graphite, Ag_2GeS_3-glass is the fast purely Ag^+ ions conducting electrolyte, and D is an equilibrium mixture of phases. According to the experimental data on the EMF versus temperature of each electrochemical cells, analytical equations for the Gibbs energies of $GeSb_8Te_{13}$, $GeSb_6Te_{10}$, $GeSb_4Te_7$, $GeSb_2Te_4$, $Ge_2Sb_2Te_5$, $Ge_3Sb_2Te_6$, and $Ge_4Sb_2Te_7$ compounds were obtained. The thermodynamic properties of silver-saturated tetradymite-like compounds have been calculated for the first time. A good correspondence between experimental values and structure data reported in literature has been established.

Keywords Thermoelectric materials, Layered compounds, Phase equilibria, Thermodynamic properties, EMF method

1. Introduction

In recent decades, the study of thermoelectric materials (TM) has attracted increasing attention both from an energy and environmental point of view. Thermoelectric materials provide a large variety of applications in heating, cooling, and power generation due to direct conversion of heat into electrical energy [1–3]. The efficiency of TM is defined by the figure-of-merit ZT parameter, which is $ZT = S^2\sigma T/(k_{el}+k_{lat})$, where S, σ, k_{el} and k_{lat} represent the Seebeck coefficient, electrical, electronic, and lattice vibrations conductivity, respectively [4]. Many studies in the past decades are focused on increasing of ZT values in several ways by studying the multicomponent materials. The ternary compounds with mixed layered tetradymite-like structure of the homologous series $nGeTe\cdot mSb_2Te_3$ (n, m =1–4) in the GeTe–Sb_2Te_3 system were identified as good TM [5–10].

The T–x phase diagram of the GeTe–Sb_2Te_3 system has been studied by Abrikosov et al. [11]. The formation of the following compounds was established $GeSb_4Te_7$, $GeSb_2Te_4$, and $Ge_2Sb_2Te_5$. These ternary compounds melt incongruently at 878, 888, and 903 K, respectively. Skums et al. [12] and Skoropanov et al. [13] reported that the $GeSb_4Te_7$ and $GeSb_2Te_4$ compounds melt congruently at 880 and 888 K, respectively. Later on, four additional compounds $Ge_4Sb_2Te_7$, $Ge_3Sb_2Te_6$, $GeSb_6Te_{10}$, and $GeSb_8Te_{13}$ of the homologous series

M. Moroz (✉)

Department of Chemistry and Physics, National University of Water and Environmental Engineering, 33028 Rivne, Ukraine

Department of Physical and Colloid Chemistry, Ivan Franko National University of Lviv, 79005 Lviv, Ukraine

e-mail: m.v.moroz@nuwm.edu.ua

F. Tesfaye, L. Hupa

Laboratory of Inorganic Chemistry, Johan Gadolin Process Chemistry Centre, Åbo Akademi University, 20500 Turku, Finland

P. Demchenko

Department of Inorganic Chemistry, Ivan Franko National University of Lviv, 79005 Lviv, Ukraine

M. Prokhorenko

Department of Cartography and Geospatial Modeling, Lviv Polytechnic National University, 79013 Lviv, Ukraine

D. Lindberg

School of Chemical Engineering, Aalto University, 02150 Espoo, Finland

O. Reshetnyak

Department of Physical and Colloid Chemistry, Ivan Franko National University of Lviv, 79005 Lviv, Ukraine

nGeTe·mSb$_2$Te$_3$ were found [5–9]. These compounds were identified by high-resolution electron microscopy, electronic diffraction [5, 6, 14, 15] and X-ray diffraction [8, 14] techniques. In the layered ternary compounds Te atoms form a cubic close packing structure with octahedral voids, occupied by Ge and Sb atoms. The hexagonal unit cells are formed by multilayer packets of different types, ordered in alternating directions in the direction perpendicular to hexagonal c axis. The layered compounds can be divided in two groups, based on the compositional variations of "GeSb$_2$Te$_4$". The structures of the GeTe-rich compounds are formed by identical slabs. The structures of Sb$_2$Te$_3$-rich compounds include five- and seven-layer slabs [8].

For the practical application of compounds in electronic cooling devices and transformation of thermal energy into electrical power, absence of structural transformations in the operating temperature range is important. Shelimova et al. [9] measured the Hall coefficient, electrical resistivity, and thermoelectric power of compounds of the homologous series in the range of 100–600 K. According to Skums et al. [12], some of these compounds undergoes a phase transition at $T > 600$ K. Below $T = 600$ K, the energy of thermal vibrations of atoms may not be sufficient to change the lattice crystal structure. Under these conditions, the phase will be in a metastable state. The examples of transition of compounds from the metastable to the thermodynamic equilibrium state were published in several works [16–21]. Such transition was carried out by including compound as one of the components into a positive electrode of the electrochemical cells (ECCs). A key role in achieving the thermodynamic equilibrium state of the compounds belongs to Ag$^+$ ions migrated from the Ag-reference electrode to multi-phase mixture of a positive electrode [22].

Moroz and Prokhorenko [16] reported that continuous solid solution of the PbSe–PbTe system at $T < 570$ K is a metastable. Decomposition of the solid solution and formation in the right electrode of ECC the intermediate phase in the PbSe$_{0.70}$Te$_{0.30}$–Pb$_{0.73}$Te$_{0.27}$ concentration range was established.

Formation of the Ag$_2$GeSe$_3$ compound in the Ag$_2$Se–GeSe$_2$ system was found under carefully controlled conditions in ECC [17]. Furthermore, Ag$_2$GeSe$_3$ was observed to undergo a phase transition at $T = 535$ K.

The phase diagram of the Bi–Te system in the entire composition range is given in [19]. It is characterized by the presence of Bi$_2$Te$_3$, Bi$_4$Te$_5$, Bi$_8$Te$_9$, BiTe, Bi$_6$Te$_5$, Bi$_4$Te$_3$, Bi$_2$Te, and Bi$_{14}$Te$_6$ compounds. Data on the temperature and concentration ranges of stability of the Bi$_2$Te$_3$, BiTe, Bi$_2$Te, and Bi$_{14}$Te$_6$ compounds are given in Abrikosov et al. [20]. It was found that BiTe and Bi$_2$Te are phases of variable composition. The phase equilibria of the Ag–Bi–Te system and thermodynamic properties of the compounds have been investigated by the electromotive force (EMF) method in the temperature range of 490–550 K [18]. It is characterized by the presence of the Ag$_2$Te–Bi, Ag$_2$Te–Bi$_{14}$Te$_6$, Ag$_2$Te–Bi$_2$Te, Ag$_2$Te–BiTe, and Ag$_2$Te–Bi$_2$Te$_3$ quasi-binary sections. A good agreement between calculated [18] and literature [23] thermodynamic data for BiTe and Bi$_2$Te$_3$ compounds confirm the phase equilibria of the Ag–Bi–Te system presented in [18]. It is mean that in thermodynamic equilibrium BiTe and Bi$_2$Te are stochiometric compounds due to the decomposition of their solid solutions under potential-forming process.

According to [21], the solid solubility of PbS in Ag$_8$GeS$_6$ does not exceed 13 mol% . Metastable state of this solid solution was established by the EMF method in [24]. It was found that maximum solubility occurs up to 19 mol% PbS. Furthermore, existence of intermediate phase with the approximated composition Ag$_{6.62}$Pb$_{0.16}$Ge$_{0.84}$S$_{5.20}$ was predicted.

Herein we present the thermodynamic properties of the saturated solid solutions of the nGeTe·mSb$_2$Te$_3$ compounds in the phase region Ag$_8$GeTe$_6$–Ge–Ge$_4$Sb$_2$Te$_7$–Sb$_2$Te$_3$ of the Ag–Ge–Sb–Te system. These thermochemical data of the compounds can be used to optimize or complete phase diagrams in the investigated system and for selection of thermodynamically stable materials with optimal values of the ZT parameter.

2. Experimental Section

The starting materials for synthesis were high-purity elements: Ag, 99.99 wt% (Alfa-Aesar, Germany); Ge, 99.999 wt% (Alfa-Aesar, Germany); Sb, 99.99 wt% (Alfa-Aesar, Germany); S, 99.999 wt% (Alfa-Aesar, Germany); Te, 99.999 wt% (Alfa-Aesar, Germany).

For the EMF measurements [24–29], the following electrochemical cell was used:

$$(-) \ C \mid Ag \mid Ag_2GeS_3\text{-glass} \mid D \mid C \ (+),$$

where C is graphite, Ag$_2$GeS$_3$-glass is the fast purely Ag$^+$ ions conducting electrolyte [30, 31], and D is an four-element equilibrium mixture of phases. The vertical lines in ECC indicate phase boundaries or contacts between cell components. The cell polarities and half-cell reactions in the ECCs were established according to rules described in [24, 32].

The positive (right) electrodes D of the EECs were synthesized by melting of chemical elements in thin-walled evacuated quartz glass ampoules at $T = 1070$ K for 5 h. Slowly cooled to room temperature samples were ground into a fine powder with the particle size of ≤ 5 µm, evacuated, and then annealing at $T = 550$ K for 250 h. The composition of positive electrodes of ECCs were calculated based on equations of electrochemical reactions for each of 7 four-phase regions of the Ag$_8$GeTe$_6$–Ge–Ge$_4$Sb$_2$Te$_7$–Sb$_2$Te$_3$ system. The Ag$_2$GeS$_3$-glass [30, 33] was obtained by melt quenching of the corresponding elements from $T = 1200$ K in ice water. The phase compositions of the right electrode compounds were characterized by differential thermal analysis (Paulik-

Paulik-Erdey derivatograph fitted with chromel-alumel thermocouples and an H307-1 XY recorder) and by X-ray powder diffraction (STOE STADI P diffractometer, transmission mode, Cu$K\alpha_1$ radiation, a bent Ge (111) monochromator on primary beam, $2\theta/\omega$ scan mode) techniques. X-ray phase analysis was performed using STOE WinXPOW [34] and PowderCell [35] program packages using crystallographic data on the structures of known phases taken from databases [36, 37].
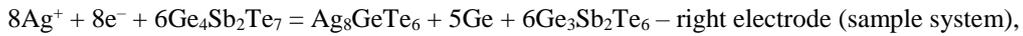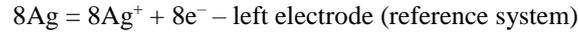
Components of the ECCs in powder form were pressed at 10^8 Pa through a 2 mm diameter hole arranged in the fluoroplast matrix up to density $\rho = (0.93 \pm 0.02) \cdot \rho_0$, where ρ_0 is the experimentally determined density of cast samples. Five-fold thermal cycling of ECCs in the temperature range of 450–510 K was performed to eliminate possible defects due to plastic deformation during sample pressing. The heating and cooling rates were of 2 K min^{-1}. Experiments were performed in a horizontal resistance furnace, similar to that described in [38]. As protective atmosphere, we used a continuously flowing highly purified (0.9999 volume fraction) Ar(g) at $P = 1.2 \cdot 10^5$ Pa, with a flow rate of $2 \cdot 10^{-3}$ m^3 h^{-1} from the right to left electrode of the ECCs. The temperature was maintained with an accuracy of ± 0.5 K. The EMF of the cells were measured by high-resistance (input impedance of $>10^{12}$ Ω) universal U7-9 digital voltmeter. The equilibrium in ECCs at each temperature was achieved within 2 h. After equilibrium has been attained, the EMF values were constant or their variation did not exceed ± 0.2 mV.

In our previous works [39, 40] we have described in details the scheme of ECCs and procedure of the EMF measurements.
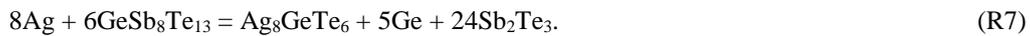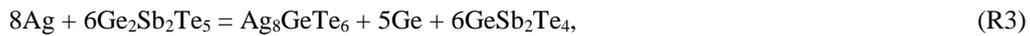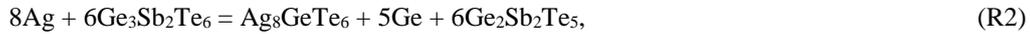
3. Results and Discussion

As can be seen in Table 1 and Fig. 1, concentration space of the Ag–Ge–Sb–Te system in the Ag$_8$GeTe$_6$–Ge–Ge$_4$Sb$_2$Te$_7$–Sb$_2$Te$_3$ part consists of 7 four-phase regions. In Fig. 1, the phase regions borders are marked by two-phase equilibrium lines. The lines of two-phase equilibria were determined in [9, 41, 42] as well as by our investigation by the EMF method. The spatial location of the established phase regions relative to composition of Ag were used to determine the thermodynamic properties of ternary compounds.

In the phase region (1), listed in Table 1, the electrochemical process of the formation of Ag$_8$GeTe$_6$, Ge, and Ge$_3$Sb$_2$Te$_6$ from the pure Ag and Ge$_4$Sb$_2$Te$_7$ compound follows:

$$8Ag = 8Ag^+ + 8e^- - \text{left electrode (reference system)}$$

$$8Ag^+ + 8e^- + 6Ge_4Sb_2Te_7 = Ag_8GeTe_6 + 5Ge + 6Ge_3Sb_2Te_6 - \text{right electrode (sample system)},$$

$$8Ag + 6Ge_4Sb_2Te_7 = Ag_8GeTe_6 + 5Ge + 6Ge_3Sb_2Te_6 - \text{overall cell reaction}. \tag{R1}$$

For the phase regions (2)–(7), listed in Table 1, the overall cell reactions can be expressed as:

$$8Ag + 6Ge_3Sb_2Te_6 = Ag_8GeTe_6 + 5Ge + 6Ge_2Sb_2Te_5, \tag{R2}$$

$$8Ag + 6Ge_2Sb_2Te_5 = Ag_8GeTe_6 + 5Ge + 6GeSb_2Te_4, \tag{R3}$$

$$8Ag + 12GeSb_2Te_4 = Ag_8GeTe_6 + 5Ge + 6GeSb_4Te_7, \tag{R4}$$

$$8Ag + 18GeSb_4Te_7 = Ag_8GeTe_6 + 5Ge + 12GeSb_6Te_{10}, \tag{R5}$$

$$8Ag + 24GeSb_6Te_{10} = Ag_8GeTe_6 + 5Ge + 18GeSb_8Te_{13}, \tag{R6}$$

$$8Ag + 6GeSb_8Te_{13} = Ag_8GeTe_6 + 5Ge + 24Sb_2Te_3. \tag{R7}$$

Reactions (R1)–(R7) were realized to take place in the ECCs at different temperatures. Based on equations (R1)–(R7), the positive electrodes D of ECCs were prepared from pure elements Ag, Ge, Sb, and Te taken in molar ratios: 1) 8 : 3 : 10 : 22, 2) 8 : 4 : 14 : 29, 3) 8 : 4 : 10 : 23, 4) 8 : 4 : 6 : 17, 5) 8 : 5 : 4 : 15, 6) 8 : 7 : 4 : 17, and 7) 8 : 9 : 4 : 19, respectively.

Table 1 Four-phase regions of the Ag–Ge–Sb–Te system in the Ag$_8$GeTe$_6$–Ge–Ge$_4$Sb$_2$Te$_7$–Sb$_2$Te$_3$ part and the EMF values of ECCs at T=480 K in corresponding phase areas

No	Phase region	E / mV
1	Ge$_4$Sb$_2$Te$_7$–Ge–Ag$_8$GeTe$_6$–Ge$_3$Sb$_2$Te$_6$	275.09
2	Ge$_3$Sb$_2$Te$_6$–Ge–Ag$_8$GeTe$_6$–Ge$_2$Sb$_2$Te$_5$	272.44
3	Ge$_2$Sb$_2$Te$_5$–Ge–Ag$_8$GeTe$_6$–GeSb$_2$Te$_4$	270.17
4	GeSb$_2$Te$_4$–Ge–Ag$_8$GeTe$_6$–GeSb$_4$Te$_7$	265.98
5	GeSb$_4$Te$_7$–Ge–Ag$_8$GeTe$_6$–GeSb$_6$Te$_{10}$	258.38
6	GeSb$_6$Te$_{10}$–Ge–Ag$_8$GeTe$_6$–GeSb$_8$Te$_{13}$	254.52
7	GeSb$_8$Te$_{13}$–Ge–Ag$_8$GeTe$_6$–Sb$_2$Te$_3$	247.50
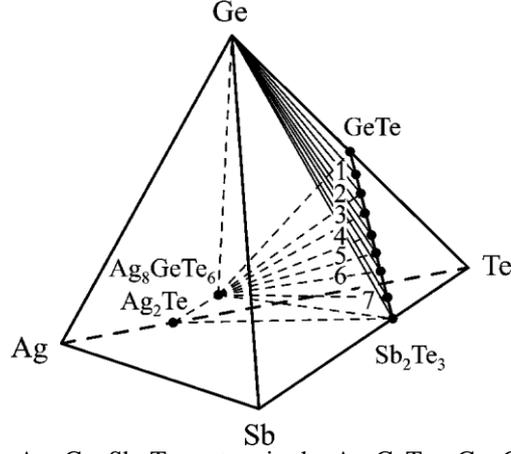
Fig. 1 The phase equilibria of the Ag–Ge–Sb–Te system in the Ag_8GeTe_6–Ge–GeTe–Sb_2Te_3 part, below $T = 520$ K. 1 is $Ge_4Sb_2Te_7$, 2 is $Ge_3Sb_2Te_6$, 3 is $Ge_2Sb_2Te_5$, 4 is $GeSb_2Te_4$, 5 is $GeSb_4Te_7$, 6 is $GeSb_6Te_{10}$, 7 is $GeSb_8Te_{13}$

The relationship of EMF versus temperature of reactions (R1)–(R7) in ECCs were approximated by Eqs. (1)–(7) and are shown in Fig. 2. The crystal lattices of tetrademite-like compounds are highly disordered, due to the presence of mixed occupancy of cations in octahedral voids [43]. The bends of the curves at different temperatures in Fig. 2 arises from individual activation changes of occupancy sites by Ge, Sb, and Ag cations that are characteristic of each of the studied phases.

$$E_{(1)}/mV = (162.98\pm0.21) + (233.56\pm0.43)\cdot10^{-3}T/K \quad 462 \leq T/K \leq 503, \tag{1}$$

$$E_{(2)}/mV = (171.25\pm0.21) + (210.82\pm0.44)\cdot10^{-3}T/K \quad 458 \leq T/K \leq 495, \tag{2}$$

$$E_{(3)}/mV = (185.46\pm0.16) + (176.48\pm0.34)\cdot10^{-3}T/K \quad 457 \leq T/K \leq 499, \tag{3}$$

$$E_{(4)}/mV = (139.20\pm0.17) + (264.13\pm0.35)\cdot10^{-3}T/K \quad 460 \leq T/K \leq 499, \tag{4}$$

$$E_{(5)}/mV = (139.39\pm0.18) + (247.89\pm0.38)\cdot10^{-3}T/K \quad 457 \leq T/K \leq 496, \tag{5}$$

$$E_{(6)}/mV = (147.71\pm0.22) + (222.53\pm0.46)\cdot10^{-3}T/K \quad 465 \leq T/K \leq 501, \tag{6}$$

$$E_{(7)}/mV = (145.75\pm0.19) + (211.97\pm0.39)\cdot10^{-3}T/K \quad 465 \leq T/K \leq 497. \tag{7}$$
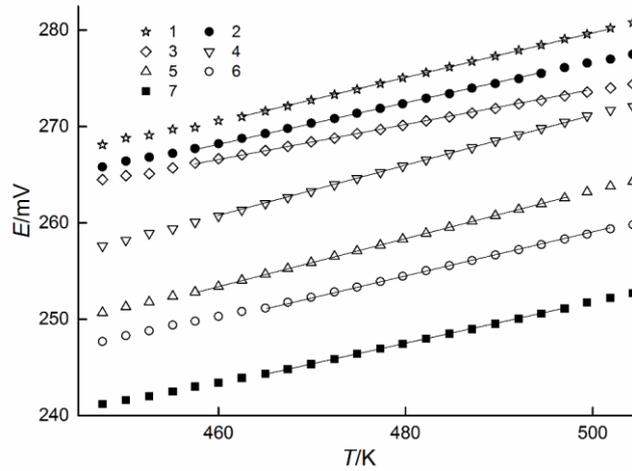
Fig. 2 The temperature dependences of EMF of the cells with the positive electrodes D of the phase regions: 1 is $Ge_4Sb_2Te_7$–Ge–Ag_8GeTe_6–$Ge_3Sb_2Te_6$, 2 is $Ge_3Sb_2Te_6$–Ge–Ag_8GeTe_6–$Ge_2Sb_2Te_5$, 3 is $Ge_2Sb_2Te_5$–Ge–Ag_8GeTe_6–$GeSb_2Te_4$, 4 is $GeSb_2Te_4$–Ge–Ag_8GeTe_6–$GeSb_4Te_7$, 5 is $GeSb_4Te_7$–Ge–Ag_8GeTe_6–$GeSb_6Te_{10}$, 6 is $GeSb_6Te_{10}$–Ge–Ag_8GeTe_6–$GeSb_8Te_{13}$, 7 is $GeSb_8Te_{13}$–Ge–Ag_8GeTe_6–Sb_2Te_3

In addition, Eqs. (1)–(7) confirm the correctness of the spatial location of the established phase regions. In particular, EMF values of ECCs remain constant independent of the general composition in the phase region, but change drastically on their boundaries [24]. Furthermore, as can be seen in Table 1, the phase region further away from the composition of Ag is characterized by higher EMF value at T=const.

The Gibbs energies, entropies, and enthalpies of the reactions (R1)–(R7) can be calculated by combining the measured EMF values of each ECC and the thermodynamic Eqs. (8)–(10) [49,59,60]:

$$\Delta_r G = -n \cdot F \cdot E, \tag{8}$$
$$\Delta_r H = -n \cdot F \cdot [E - (dE/dT)T], \tag{9}$$
$$\Delta_r S = n \cdot F \cdot (dE/dT), \tag{10}$$

where $n = 8$ is the number of electrons involved in the reactions (R1)–(R7), $F = 96485.33289$ C·mol^{-1} is Faraday constant, and E is the EMF of the electrochemical cells.

By assuming $\left(\frac{\partial \Delta_r H}{\partial T}\right)_p = 0$ and $\left(\frac{\partial \Delta_r S}{\partial T}\right)_p = 0$, which implies that $\Delta_r C_p = 0$ [32], the thermodynamic function of reactions (R1)–(R7) were calculated through extrapolation of the linear temperature dependences of the EMF of ECCs to $T = 298$ K and using Eqs. (8)–(10). The results of the calculations are listed in Table 2.

Table 2 Standard thermodynamic values of reactions (R1)–(R7) in ECCs at $T = 298$ K

Reaction	$-\Delta_r G^\circ$	$-\Delta_r H^\circ$	$\Delta_r S^\circ$
	kJ·mol^{-1}		J·mol^{-1}·K^{-1}
(R1)	179.53 ± 0.62	125.80 ± 0.16	180.28 ± 0.33
(R2)	180.68 ± 0.66	132.18 ± 0.16	162.73 ± 0.34
(R3)	183.75 ± 0.57	143.15 ± 0.12	136.22 ± 0.26
(R4)	168.20 ± 0.48	107.45 ± 0.13	203.88 ± 0.27
(R5)	164.61 ± 0.52	107.59 ± 0.14	191.34 ± 0.29
(R6)	165.20 ± 0.64	114.01 ± 0.17	171.77 ± 0.36
(R7)	161.26 ± 0.56	112.50 ± 0.15	163.62 ± 0.30

Standard Gibbs energy and entropy of reactions (R1)–(R7) are related to the Gibbs energy of formation and entropy of compounds and pure elements the following equations:

$$\Delta_{r(1)}G^\circ = \Delta_f G^\circ_{Ag_8GeTe_6} + 6\Delta_f G^\circ_{Ge_3Sb_2Te_6} - 6\Delta_f G^\circ_{Ge_4Sb_2Te_7}, \tag{11}$$

$$\Delta_{r(1)}S^\circ = S^\circ_{Ag_8GeTe_6} + 5S^\circ_{Ge} + 6S^\circ_{Ge_3Sb_2Te_6} - 8S^\circ_{Ag} - 6S^\circ_{Ge_4Sb_2Te_7}, \tag{12}$$

$$\Delta_{r(2)}G^\circ = \Delta_f G^\circ_{Ag_8GeTe_6} + 6\Delta_f G^\circ_{Ge_2Sb_2Te_5} - 6\Delta_f G^\circ_{Ge_3Sb_2Te_6}, \tag{13}$$

$$\Delta_{r(2)}S^\circ = S^\circ_{Ag_8GeTe_6} + 5S^\circ_{Ge} + 6S^\circ_{Ge_2Sb_2Te_5} - 8S^\circ_{Ag} - 6S^\circ_{Ge_3Sb_2Te_6}, \tag{14}$$

$$\Delta_{r(3)}G^\circ = \Delta_f G^\circ_{Ag_8GeTe_6} + 6\Delta_f G^\circ_{GeSb_2Te_4} - 6\Delta_f G^\circ_{Ge_2Sb_2Te_5}, \tag{15}$$

$$\Delta_{r(3)}S^\circ = S^\circ_{Ag_8GeTe_6} + 5S^\circ_{Ge} + 6S^\circ_{GeSb_2Te_4} - 8S^\circ_{Ag} - 6S^\circ_{Ge_2Sb_2Te_5}, \tag{16}$$

$$\Delta_{r(4)}G^\circ = \Delta_f G^\circ_{Ag_8GeTe_6} + 6\Delta_f G^\circ_{GeSb_4Te_7} - 12\Delta_f G^\circ_{GeSb_2Te_4}, \tag{17}$$

$$\Delta_{r(4)}S^\circ = S^\circ_{Ag_8GeTe_6} + 5S^\circ_{Ge} + 6S^\circ_{GeSb_4Te_7} - 8S^\circ_{Ag} - 12S^\circ_{GeSb_2Te_4}, \tag{18}$$

$$\Delta_{r(5)}G^\circ = \Delta_f G^\circ_{Ag_8GeTe_6} + 12\Delta_f G^\circ_{GeSb_6Te_{10}} - 18\Delta_f G^\circ_{GeSb_4Te_7}, \tag{19}$$

$$\Delta_{r(5)}S^\circ = S^\circ_{Ag_8GeTe_6} + 5S^\circ_{Ge} + 12S^\circ_{GeSb_6Te_{10}} - 8S^\circ_{Ag} - 18S^\circ_{GeSb_4Te_7}, \tag{20}$$

$$\Delta_{r(6)}G^\circ = \Delta_f G^\circ_{Ag_8GeTe_6} + 18\Delta_f G^\circ_{GeSb_8Te_{13}} - 24\Delta_f G^\circ_{GeSb_6Te_{10}}, \tag{21}$$

$$\Delta_{r(6)}S^\circ = S^\circ_{Ag_8GeTe_6} + 5S^\circ_{Ge} + 18S^\circ_{GeSb_8Te_{13}} - 8S^\circ_{Ag} - 24S^\circ_{GeSb_6Te_{10}}, \tag{22}$$

$$\Delta_{r(7)}G^\circ = \Delta_f G^\circ_{Ag_8GeTe_6} + 24\Delta_f G^\circ_{Sb_2Te_3} - 6\Delta_f G^\circ_{GeSb_8Te_{13}}, \tag{23}$$

$$\Delta_{r(7)}S^\circ = S^\circ_{Ag_8GeTe_6} + 5S^\circ_{Ge} + 24S^\circ_{Sb_2Te_3} - 8S^\circ_{Ag} - 6S^\circ_{GeSb_8Te_{13}}. \tag{24}$$

The entropy of formations of the GeSb$_8$Te$_{13}$ compound can be calculated as:

$$\Delta_f S^\circ_{GeSb_8Te_{13}} = S^\circ_{GeSb_8Te_{13}} - S^\circ_{Ge} - 8S^\circ_{Sb} - 13S^\circ_{Te}. \tag{25}$$

For Ge$_3$Sb$_2$Te$_6$, Ge$_4$Sb$_2$Te$_7$, Ge$_2$Sb$_2$Te$_5$, GeSb$_2$Te$_4$, GeSb$_4$Te$_7$, and GeSb$_6$Te$_{10}$ compounds the corresponding reactions to determine $\Delta_f S^\circ$ can be written similar to Eq. (25) with their respective moles.

By combining Eqs. (8)–(25) and using data of the pure elements [23], Ag$_8$GeTe$_6$, and Sb$_2$Te$_3$ [23, 24], the standard Gibbs energy of formations of the layered tetradymite-like compounds of the homologous series nGeTe·mSb$_2$Te$_3$ were calculated to be:

$$\Delta_f G^\circ_{GeSb_8Te_{13}}/(kJ·mol^{-1}) = -(248.06 \pm 2.17) - (3.90 \pm 0.03) \cdot 10^{-3}T/K, \tag{26}$$

$$\Delta_f G^{\circ}_{\text{GeSb}_6\text{Te}_{10}}/(\text{kJ·mol}^{-1}) = -(191.51 \pm 1.56) - (1.74 \pm 0.02) \cdot 10^{-3}T/\text{K}, \tag{27}$$

$$\Delta_f G^{\circ}_{\text{GeSb}_4\text{Te}_7}/(\text{kJ·mol}^{-1}) = -(135.32 \pm 1.01) + (0.75 \pm 0.01) \cdot 10^{-3}T/\text{K}, \tag{28}$$

$$\Delta_f G^{\circ}_{\text{GeSb}_2\text{Te}_4}/(\text{kJ·mol}^{-1}) = -(79.14 \pm 0.53) + (3.54 \pm 0.02) \cdot 10^{-3}T/\text{K}, \tag{29}$$

$$\Delta_f G^{\circ}_{\text{Ge}_2\text{Sb}_2\text{Te}_5}/(\text{kJ·mol}^{-1}) = -(96.16 \pm 1.21) + (6.50 \pm 0.06) \cdot 10^{-3}T/\text{K}, \tag{30}$$

$$\Delta_f G^{\circ}_{\text{Ge}_3\text{Sb}_2\text{Te}_6}/(\text{kJ·mol}^{-1}) = -(114.99 \pm 2.13) + (10.79 \pm 0.16) \cdot 10^{-3}T/\text{K}, \tag{31}$$

$$\Delta_f G^{\circ}_{\text{Ge}_4\text{Sb}_2\text{Te}_7}/(\text{kJ·mol}^{-1}) = -(134.90 \pm 3.29) + (15.96 \pm 0.31) \cdot 10^{-3}T/\text{K}. \tag{32}$$

The thermodynamic values of the saturated solid solutions of compounds in the Ag_8GeTe_6–Ge–$Ge_4Sb_2Te_7$–Sb_2Te_3 part are given in Table 3 and Fig. 3.

Table 3 Summary of the standard thermodynamic properties of layered tetradymite-like compounds of the GeTe–Sb_2Te_3 system at T=298 K determined in this work

Phase	$-\Delta_f G^{\circ}$	$-\Delta_f H^{\circ}$	$T\Delta_f S^{\circ}$	S°	$\Delta_f S^{\circ}$
	kJ·mol^{-1}			J·mol^{-1}·K^{-1}	
$GeSb_8Te_{13}$	251.96±1.38	248.06±2.17	3.90±0.03	1051.80±14.73	13.09±0.09
$GeSb_6Te_{10}$	193.25±1.28	191.51±1.56	1.74±0.02	805.02±13.61	5.84±0.04
$GeSb_4Te_7$	134.57±1.18	135.32±1.01	−0.75±0.01	557.16±6.48	−2.50±0.02
$GeSb_2Te_4$	75.60±1.09	79.14±0.53	−3.54±0.02	308.25±3.35	−11.88±0.06
$Ge_2Sb_2Te_5$	89.66±1.21	96.16±1.21	−6.50±0.06	378.86±3.34	−21.84±0.21
$Ge_3Sb_2Te_6$	104.20±1.38	114.99±2.13	−10.79±0.16	445.06±5.91	−36.23±0.53
$Ge_4Sb_2Te_7$	118.94±1.57	134.90±3.29	−15.96±0.31	508.32±8.99	−53.54±1.03
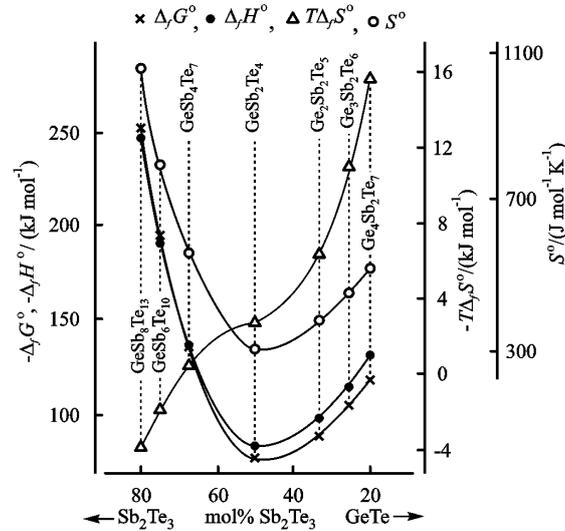
Fig. 3 Concentration changes of thermodynamic functions of layered tetradymite-like compounds of the GeTe–Sb_2Te_3 system

As can been seen in Fig. 3, at 50 mol% Sb_2Te_3, a composition that corresponds to $GeSb_2Te_4$ compound, the $\Delta_f G^{\circ}$, $\Delta_f H^{\circ}$, S° values are minimum and the sign of the second derivative of $T\Delta_f S^{\circ}$ function changes. Gibbs energy, enthalpy, and entropy of the compounds is observed to increase with the addition of GeTe or Sb_2Te_3 to $GeSb_2Te_4$ composition. Results shown in Table 3 and Fig. 3 are in a good agreement with those data reported in [7–9] regarding the difference in the crystal structures of the compounds of the GeTe–Sb_2Te_3 system on either side of the $GeSb_2Te_4$. The unit cell of the $GeSb_2Te_4$ compound contains 3 seven-layer slabs across the c axis. According to [7], in GeTe-rich compounds thermodynamic values increasing is accounted with more quantities of atomic layers in the packet and number of the same type packets that determine the unit cell parameter c. For the Sb_2Te_3-rich compounds, increases are due to the number and alternation of 5- and 7-layer packets along the c axis.

4. Conclusions

1. The reproducibility of the values $E_{(1)-(7)}(T)$ of the ECCs during the heating and cooling cycles characterizes saturated solid solutions of the compounds of the GeTe–Sb$_2$Te$_3$ system as thermodynamically stable phases in the temperature range of 455–505 K.
2. The measured EMF values were applied to calculate the Gibbs energies, enthalpies, and entropies of silver-saturated solid solutions of the nGeTe·mSb$_2$Te$_3$ (n, m =1–4) compounds.
3. Concentration dependences of the thermodynamic values of compounds confirm the previously established difference between the crystalline structures of GeTe-rich and Sb$_2$Te$_3$-rich phases of the GeTe–Sb$_2$Te$_3$ system.

Acknowledgements

Conflict of Interest

The authors declare that they have no conflict of interest.

References

1. Rogacheva EI, Nashchekina ON, Tavrina TV, Vekhov YeO, Sipatov AYu, Dresselhaus MS (2003) Non-stoichiometry in SnTe thin films and temperature instabilities of thermoelectric properties. Mater. Sci. Semicond. Process. 6(5–6):497–501
2. Rogacheva EI, Nashchekina ON, Sipatov AYu, Fedorov AG, Grigorov SN (2009) Growth mechanism and thermoelectric properties of PbSe/EuS superlattices. Phys. Status Solidi C. 6(5):1149–1153
3. Chu S, Majumdar A (2012) Opportunities and challenges for a sustainable energy future. Nature 488(7411):294–303
4. Tesfaye F, Moroz M (2018) An Overview of Advanced Chalcogenide Thermo-electric Materials and Their Applications. J. Electron. Res. Appl. 2(2):28–41
5. Kuypers S, van Tendeloo G, van Landuyt J, Amelinckx S (1988) Electron microscopic study of the homologous series of mixed layer compounds R$_2$Te$_3$(GeTe)$_n$ (R = Sb, Bi). J. Solid State Chem. 76(1):102–108
6. Frangis N, Kuypers S, Manolikas C, Van Landuyt J, Amelinckx S (1989) Continuous series of one-dimensional structures in the compounds Bi$_{2+x}$Se$_3$, Bi$_{2+x}$Te$_3$, Sb$_{2+x}$Te$_3$, (Bi$_2$Te$_3$)$_n$GeTe and (Sb$_2$Te$_3$)$_n$GeTe. Solid State Commun. 69(8):817–819
7. Shelimova LE, Karpinskii OG, Zemskov VS, Konstantinov PP (2000) Structural and electrical properties of layered tetradymite-like compounds in the GeTe—Bi$_2$Te$_3$ and GeTe—Sb$_2$Te$_3$ systems. Inorg. Mater. 36(3):235–242
8. Shelimova LE, Karpinskii OG, Kretova MA, Kosyakov VI, Shestakov VA (2000) Homologous series of layered tetradymite-like compounds in the Sb-Te and GeTe-Sb$_2$Te$_3$ systems. Inorg. Mater. 36(8):768–775
9. Shelimova LE, Karpinskii OG, Konstantinov PP, Kretova MA, Avilov ES, Zemskov VS (2001) Composition and Properties of Layered Compounds in the GeTe–Sb$_2$Te$_3$ System. Inorg. Mater. 37(4):342–348
10. Horichok I, Ahiska R, Freik D, Nykyruy L, Mudry S (2016) Phase Content and Thermoelectric Properties of Optimized Thermoelectric Structures Based on the Ag-Pb-Sb-Te System. J. Electron. Mater. 45(3):1576–1583
11. Abrikosov NK, Danilova-Dobryakova GT (1965) Sb$_2$Te$_3$-GeTe Phase Diagram. Izv Akad Nauk SSSR Neorg. Mater. 1(2):204–209 (in Russian)
12. Skums VF, Valevskii BL, Pashko VA (1985) Quantitative Differential Thermal Analysis of Phase Relations in the GeTe-Sb$_2$Te$_3$ System. Zh Fiz Khim. 59(9):2159–2162
13. Skoropanov AS, Valevsky BL, Skums VF, Samal GI, Vecher AA (1985) Physico-chemical study of Ge(Pb)Te-Bi$_2$(Sb$_2$)Te$_3$ system ternary compounds. Thermochim. Acta. 90:331–334
14. Karpinsky OG, Shelimova LE, Kretova MA, Fleurial J-P (1998) An X-ray study of the mixed-layered compounds of (GeTe)$_n$ (Sb$_2$Te$_3$)$_m$ homologous series. J. Alloys Compd. 268(1–2):112–117
15. Karpinskii OG, Shelimova LE, Kretova MA, Fleurial JP (1998) Structural Study of Ternary Layered Compounds in the (GeTe)$_n$·(Bi$_2$Te$_3$)$_m$ and (GeTe)$_n$·(Sb$_2$Te$_3$)$_m$ Homologous Series. Inorg. Mater. 34(3):225–232
16. Moroz MV, Prokhorenko MV (2015) Phase relations in PbSe-PbTe alloys of the Ag-Pb-Se-Te system studied by EMF measurements. Inorg. Mater. 51(4):302–306
17. Moroz MV, Prokhorenko MV (2015) Determination of thermodynamic properties of saturated solid solutions of the Ag–Ge–Se system using EMF technique. Russ. J. Electrochem. 51(7):697–702

18. Prokhorenko MV, Moroz MV, Demchenko PYu (2015) Measuring the thermodynamic properties of saturated solid solutions in the Ag_2Te-Bi-Bi_2Te_3 system by the electromotive force method. Russ. J. Phys. Chem. A. 89(8):1330–1334

19. Shelimova LE, Karpinsky OG, Kretova MA, Avilov ES (1996) Phase equilibria in the Ge-Bi-Te ternary system at 570–770 K temperature range. J. Alloys Compd. 243(1–2):194–201

20. Abrikosov NKh, Stasova MM (1985) Solid solutions based on bismuth and antimony tellurides and bismuth selenides. Izv Akad Nauk SSSR Neorg. Mater. 21(12):2011–2015 (in Russian)

21. Moroz MV, Demchenko PYu, Prokhorenko MV, Reshetnyak OV (2017) Thermodynamic Properties of Saturated Solid Solutions of the Phases Ag_2PbGeS_4, $Ag_{0.5}Pb_{1.75}GeS_4$ and $Ag_{6.72}Pb_{0.16}Ge_{0.84}S_{5.20}$ of the Ag-Pb-Ge-S System Determined by EMF Method. J. Phase Equilibria Diffus. 38(4):426–433

22. Karapetyans MKh (1953) Chemical thermodynamics. Goskhimizdat, Moscow (in Russian)

23. Barin I (1995) Thermochemical data of pure substance. VCH, Weinheim

24. Babanly, MB, Yusibov, YA, Babanly, NB (2011) The EMF method with solid-state electrolyte in the thermodynamic investigation of ternary copper and silver chalcogenides. In: Kara, S (ed) Electromotive Force and Measurement in Several Systems. InTech, p 57-78

25. Voronin MV, Osadchii EG (2013) Thermodynamic properties of silver and bismuth sulfosalt minerals, pavonite ($AgBi_3S_5$) and matildite ($AgBiS_2$) and implications for ore deposits. Econ. Geol. 108(5):1203–1210

26. Aliev ZS, Musayeva SS, Imamaliyeva SZ, Babanly MB (2017) Thermodynamic study of antimony chalcoiodides by EMF method with an ionic liquid. J. Therm. Anal. Calorim. 133:1115–1120

27. Voronin MV, Osadchii EG, Brichkina EA (2017) Thermochemical properties of silver tellurides including empressite (AgTe) and phase diagrams for Ag–Te and Ag–Te–O. Phys. Chem. Miner. 44(9):639–653

28. Babanly NB, Orujlu EN, Imamaliyeva SZ, Yusibov YA, Babanly MB (2019) Thermodynamic investigation of silver-thallium tellurides by EMF method with solid electrolyte Ag_4RbI_5. J. Chem. Thermodyn. 128:78–86

29. Imamaliyeva SZ, Musayeva SS, Babanly DM, Jafarov YI, Taghiyev DB, Babanly MB (2019) Determination of the thermodynamic functions of bismuth chalcoiodides by EMF method with morpholinium formate as electrolyte. Thermochim. Acta. 679:178319

30. Robinel E, Carette B, Ribes M (1983) Silver sulfide based glasses (I): glass forming regions, structure and ionic conduction of glasses in GeS_2–Ag_2S and GeS_2–Ag_2S–AgI systems. J. Non-Cryst. Solids. 57(1):49–58

31. Moroz MV, Demchenko PYu, Prokhorenko SV, Moroz VM (2013) Physical properties of glasses in the Ag_2GeS_3-AgBr system. Phys. Solid State. 55(8):1613–1618

32. Osadchii EG, Rappo OA (2004) Determination of standard thermodynamic properties of sulfides in the Ag-Au-S system by means of a solid-state galvanic cell. Am. Mineral. 89(10):1405–1410

33. Moroz M, Tesfaye F, Demchenko P, Prokhorenko M, Lindberg D, Reshetnyak O, Hupa L (2018) Determination of the thermodynamic properties of the $Ag_2CdSn_3S_8$ and Ag_2CdSnS_4 phases in the Ag–Cd–Sn–S system by the solid-state electrochemical cell method. J. Chem. Thermodyn. 118:255–262

34. Diffractometer. Stoe WinXPOW, Version 3.03 (2010) Stoe Cie GmbH Darmstadt

35. Kraus W, Nolze G (1996) POWDER CELL – a program for the representation and manipulation of crystal structures and calculation of the resulting X-ray powder patterns. J. Appl. Crystallogr. 29:301–303

36. Downs RT, Hall-Wallace M (2003) The American Mineralogist crystal structure database. Am. Mineral. 88(1):247–250

37. Villars, P, Cenzual, K, (ed) (2014) Pearson's Crystal Data: Crystal Structure Database for Inorganic Compounds, Release 2014/15. ASM International, Ohio, USA

38. Tesfaye F, Taskinen P (2014) Electrochemical study of the thermodynamic properties of matildite (β-$AgBiS_2$) in different temperature and compositional ranges. J. Solid State Electrochem. 18(6):1683–1694

39. Moroz M, Tesfaye F, Demchenko P, Prokhorenko M, Lindberg D, Reshetnyak O, Hupa L (2018) Thermodynamic Properties of Magnetic Semiconductors $Ag_2FeSn_3S_8$ and Ag_2FeSnS_4 Determined by the EMF Method. In: Lambotte G, Lee J, Allanore A, Wagstaff S (ed) Materials Processing Fundamentals 2018; Springer, New York, p 87-98

40. Moroz M, Tesfaye F, Demchenko P, Prokhorenko M, Lindberg D, Reshetnyak O, Hupa L (2019) Thermal Stability and Thermodynamics of the Ag_2ZnGeS_4 Compound. In: Lambotte G, Lee J, Allanore A, Wagstaff S (ed) Materials Processing Fundamentals 2019; Springer, New York, p 215-226

41. Blachnik R, Gather B (1978) Mischungen von GeTe, SnTe und PbTe MIT Ag_2Te lin beitrag zur klärung der konstitution der ternären Ag-IVb-Te systeme (IVb = Ge, Sn, Pb). J. Common Met. 60(1):25–32

42. Wu H-J, Chen S-W (2011) Phase equilibria of Ag–Sb–Te thermoelectric materials. Acta Mater. 59(16):6463–6472

43. Shelimova LE, Karpinskii OG, Svechnikova TE, Nikhezina IYu, Avilov ES, Kretova M.A., Zemskov VS (2008) Effect of Cadmium, Silver, and Tellurium Doping on the Properties of Single Crystals of the Layered Compounds $PbBi_4Te_7$ and $PbSb_2Te_4$. Inorg. Mater. 44(4):371–376